Proceedings of the 2nd International Conference on Functional Materials and Civil Engineering
DOI: 10.54254/2755-2721/72/20241053

Damage identification of statically indeterminate trusses based on Bayesian updating

Jiangyan Liu

Eurasian International Academy, Henan University, Henan, Kaifeng, 475000, China

liujiangyan@henu.edu.cn

Abstract. Amidst China's rapid development, most structures and edifices have advanced into the mid-service life phase, where components and frameworks gradually undergo aging and deterioration. Ensuring the safety and functionality of buildings necessitates a heightened emphasis on structural health assessments. This study aims to explore a more cost-effective and time-efficient diagnostic strategy for detecting damage in statically indeterminate trusses, while exploring techniques to uphold data precision by reducing loading nodes and measurement parameters. Employing OpenSees for model construction, this paper utilizes Bayesian updating through Monte Carlo rejection sampling to pinpoint damage in statically indeterminate trusses. Moreover, it unveils the fundamental principles behind optimal loading and measurement strategies. Findings from conducted experiments advocate for a comprehensive approach integrating displacement measurements across multiple axes for enhanced accuracy, surpassing single-direction measurements. Validation of the virtual work principle underscores this method's efficacy. Ultimately, this methodology holds promise for curbing engineering expenses and amplifying operational efficiency in real scenarios.

Keywords: Bayesian updating, damage identification, structural mechanics, numerical simulation.

1. Introduction

China has consistently showcased remarkable strides in quality and development. The country's architectural landscape has witnessed an exponential surge in the number of buildings, reflecting its dynamic growth. Presently, China stands at the brink of urbanization completion, with a notable deceleration in the pace of urban construction initiatives. The urban fabric now predominantly comprises structures at the mid-service life stage, where components and frameworks have naturally succumbed to wear and tear. This degradation owes itself to myriad influences, including fluctuating temperatures and the gradual weathering of building exteriors, leading to fissures.

Furthermore, the prolonged exposure of structures to a spectrum of natural calamities and human-induced disruptions—ranging from floods and earthquakes to corrosion and explosions—can cumulatively exacerbate damage over their operational. As time elapses, the cumulative effects of these impairments contribute to the degradation of buildings and infrastructure. Subsequently, the assessment of structural integrity and safety through structural health inspections becomes imperative, facilitating preemptive repairs or replacements before structural failure occurs, thereby safeguarding the occupants and integrity of the edifice or facility [1]. Undoubtedly, the failure to promptly identify and address

DOI: 10.54254/2755-2721/72/20241053

structural damage may culminate in catastrophic building collapses, potentially resulting in substantial human casualties and property devastation [2]. It is evident, therefore, that vigilant monitoring of structural health and damage detection ensures the structure's sustained functionality and longevity and substantially diminishes the maintenance costs linked to structural upkeep [3]. In the realm of scholarly pursuit, the realm of structural health assessment equips engineers with an enriched comprehension of the stress distribution within engineering constructs, the trajectory of structural deterioration, and the fundamental principles dictating this progression. And it is vital to safeguard and reinforce the damaged components at a subsequent stage.

The quest for identifying structural damage has remained at the core of structural health evaluations. This investigative process is delineated into four hierarchical tiers, elucidated as follows [4]: 1. The initial stage entails verifying the presence of structural damage. 2. Pinpointing the precise location of the damage within the structure. 3. Gauging the magnitude of the damage at the identified site. 4. Prognosticating the residual life expectancy of the structure subsequent to damage assessment. In recent years, the evolution of methods for structural damage detection has engendered a burgeoning interest in Bayesian updating as a propitious strategy for navigating uncertainties and harnessing many information sources. This burgeoning curiosity has lent impetus to integrating this technique within the domain of civil engineering [5]. The Bayesian Theory of finite element model updating method capitalizes on a comprehensive spectrum of information sources, incorporating the assimilation of prior knowledge, refinement of prior data through field assessments, and the evaluation of structural reliability sans compromising confidence levels [6]. Many scholarly endeavors within civil engineering worldwide have delved into exploring Bayesian updating for identifying structural damage and health assessment, illuminating its potential for revolutionizing practices. For example, Simone et al. from the University of California, San Diego, delved into Bayesian linear finite element updating methodology, focusing on an experimental prototype of a seven-story steel-concrete edifice [7]. Their research aspirations centered around unraveling the intricacies of damage accrual within such structures. Meanwhile, in China, Li Quanwang and fellow researchers made substantial strides by deploying the subset simulation technique for Bayesian updating, tailored explicitly for refining intricate concrete models [8].

The primary aim of this study is to introduce a more cost-effective and streamlined diagnostic technique for detecting damage in statically indeterminate trusses. Leveraging the Bayesian updating strategy for structural damage in trusses, the model is established utilizing OpenSees, and a series of loading and point measurement trials are carried out. Computational tasks are executed through Monte Carlo rejection sampling and Bayesian updating, with data examination employing histograms, root-mean-square disparities, and other analytical tools.

2. Research Methodology

A diverse array of deterministic methodologies dominates the landscape of structural damage identification. However, a notable portion of these methodologies relies on idealized models that neglect the inherent uncertainties in reality, potentially resulting in flawed outcomes. With the evolution of civil engineering, uncertainty methodologies have emerged to enable more accurate modeling. These methodologies are bifurcated into two principal categories: non-model-based methods (NMBs) and model-based methods (MMBs), both integral for comprehensive damage identification [9]. In this study, we employ the model correction approach within the framework of modeled damage identification. Bayesian updating, coupled with Monte Carlo rejection sampling for data screening, is harnessed to enhance the precision of updating processes. Subsequently, the data undergoes analysis using the Root Mean Square Error (RMSE) difference technique. As elucidated, Bayesian updating involves refining a prior distribution using a known distribution to infer the posterior distribution [10]. This process is underpinned by constructing a likelihood function, with the preceding distribution typically rooted in engineering expertise or past data. The likelihood function quantifies the probability of an observation occurring given the parameter θ in the prior distribution. Subsequently, the posterior distribution is derived by amalgamating the prior distribution with the likelihood function. Simultaneously, Monte Carlo rejection sampling enhances sampling efficiency and accuracy. This method leverages known

DOI: 10.54254/2755-2721/72/20241053

distributions to generate samples from unknown distributions. The fundamental principle of Monte Carlo rejection sampling involves using a proposed distribution to envelop the target distribution. By comparing the proportions between the target and proposed distributions, a decision is made to accept or reject the sample. This technique guarantees that the final sample aligns with the target distribution, ensuring accuracy and reliability the sampling process. In the final analysis, the RMSE is leveraged to assess the data using the formula:

$$\left(\frac{\sum(true\ value-priori\ value)^2}{sample\ size}\right)^{-\frac{1}{2}} \tag{1}$$

RMSE is a robust metric for comparing data quality, surpassing standard deviation and other analogous measures. This metric effectively quantifies the discrepancy between measured values, making it a valuable tool for evaluating the correlation between accepted samples and a priori data across various scenarios at the culmination this experimentation.3. Experimental ProcessStyle and spacing

3. Research process

Footnotes should be avoided whenever possible. If required they should be used only for brief notes that do not fit conveniently into the text.

3.1. Research Objects

This study's analytical focus centers on statically indeterminate trusses as depicted in Figure 1. Within the simulated framework, the diagonal bar 3-8 and the crossbar 3-4 are designated as damaged elements, with their specific damage conditions remaining undisclosed. It is presumed that Bar 3-4 follows a uniform distribution with a mean value of 0.56 and a standard deviation of 1.54, while Bar 3-8 adheres to a uniform distribution with a mean value of 0.28 and a standard deviation of 1.26. The other bars in the truss possess known stiffness values as delineated in Table 1. Notably, the horizontal nodes are spaced 15 meters apart, mirroring the 15-meter separation between vertical nodes. The measurement outcomes reflect a degree of imprecision, manifested through a normal distribution with an absolute error standard deviation of 0.5 mm.

The experiment unfolds in two distinctive phases. Initially, a systematic methodology is embraced to carry out loading trials encompassing diverse configurations of nodes and loading orientations. An optimal loading strategy is deduced by scrutinizing the horizontal and vertical displacements of all nodes (excluding nodes 1 and 5, known to remain static under any loading conditions). The subsequent phase involves deriving an optimal measurement strategy based on the established loading scheme from the first phase. This entails measuring displacements at various nodes relative to different directions. Ultimately, a comprehensive synthesis of findings culminates in formulating overarching principles and conclusions for the study.

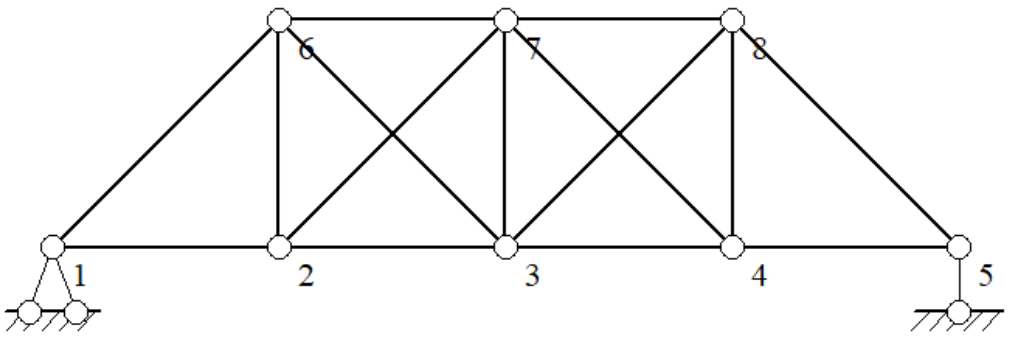

Figure 1. Experimental model

DOI: 10.54254/2755-2721/72/20241053

Table 1. Known stiffness of bars

Bar(node)	1-2	2-3	4-5	1-6	6-7	7-8	2-7
EA/105KN·m²	1.4	1.33	1.4	1.54	1.47	1.47	1.05
Bar(node)	8-5	2-6	3-6	3-7	4-8	4-7	
EA/105KN·m²	1.54	1.26	1.12	1.12	1.26	1.05	

3.2. Experimental study of static loading

To determine the optimal solution for static loading, it is imperative to eliminate extraneous variables that could impact the experiment. In the initial experiment phase, this study adopts a holistic approach by measuring all nodes' horizontal and vertical displacements. The damaged bars are presumed to retain 70% of the maximum predicted stiffness. Subsequently, the nodes undergo static loading at a magnitude of 100 KN within the model, yielding a set of a priori distribution data. Following this, a loading scheme generating 10,000 random stiffness values for bars 3-4 and 3-8 is implemented, adhering to the uniform distribution of the damaged bars. These sample data are then integrated into a likelihood function calculation, structured on a normal distribution basis. The formula:

$$e^{-\frac{\frac{1}{2}(simulated\ value-priori\ value)^2}{0.0005}} \tag{2}$$

The formula is computed post Monte Carlo rejection sampling to sieve through samples for data extraction. The output includes the count of accepted samples and the stiffness values of the bars that were accepted. Subsequently, the data is processed in Excel, and a histogram depicting the distribution of accepted data is generated for observation. The proximity of numerical values indicates the efficacy of the update process, with a stronger correspondence signifying greater effectiveness. Similarly, the resemblance of the generated image to a normal distribution serves as a barometer for the success of the update. Various loading programs were applied to the nodes to determine the optimal integrated loading scheme, and their effectiveness wasically assessed.

Initially, a static loading experiment featuring a singular load is executed alongside an evaluation encompassing the comparison of relative errors. The likelihood function is defined as

$$e^{-\frac{\frac{1}{2}(simulate\ value-\ priori\ value)^2}{0.05(\ priori\ value)^2}} \tag{3}$$

It emphasizing that the relative error amounts to 5% of the actual value. The loading scenarios entail: 1. Application of a vertical downward load with a magnitude of 100 KN. 2. Impo sition of a vertical upward load of 100 KN. 3. Placement of a horizontal leftward load totaling 100 KN. 4. Imposing a horizontal rightward load of 100 KN. Subsequent analysis delves into assessing the efficacy of each loading configuration achieving optimal outcomes.

Following the initial phase, a subsequent double-load static loading experiment was conducted, delineated into two distinctive categories: same-direction and opposite-direction configurations. This study introduces five loading schemes, veering away from comparative assessments based on relative errors. The first four loading schemes encompass 15 cases, while the fifth encompasses 30 cases. For instance, scenarios such as loading two nodes upward and three nodes downward, or vice versa, exemplify the heterogeneity in loading configurations. The loading schemes include: 1. Double vertical load, downward in the same direction, with a magnitude of 100 KN. 2. Double vertical load, upward with a force of 100 KN. The third loading scheme involves a double vertical load towards the left, exerting a load of 100 KN. Subsequently, a fourth scenario comprises a double vertical load directed to the right with a loading intensity of 100 KN. The fifth loading scheme encompasses a double vertical anisotropic load of 100 KN. Upon comprehensive analysis and comparison, the optimal loading scheme was delineated. The most effective loading strategy for the horizontal bar (3-4 bars) entailed a double vertical load in the same direction, downward loading at both node 2 and node 8. Conversely, the optimal approach for the diagonal bar (4-8 bars) involved a double vertical anisotropic loading pattern at node 3 and node 8. Figure 2 visually represents the optimal loading scheme, with the horizontal axis

DOI: 10.54254/2755-2721/72/20241053

representing stiffness (EA/10^5KN·m2) and the vertical axis denoting the frequency of acceptance. The transverse bar corresponds to the right side, indicating the inclined bar the structural configuration.

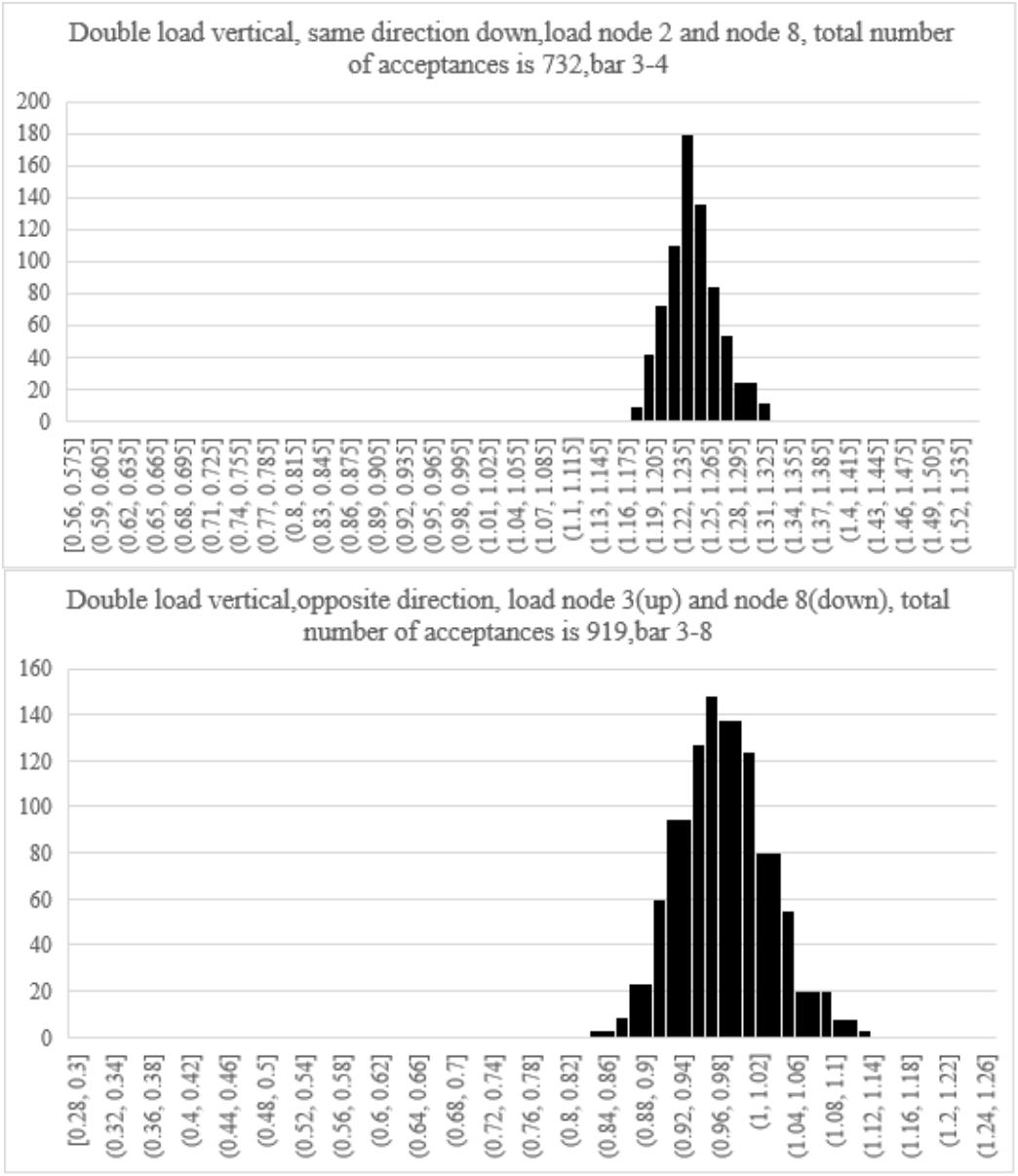

Figure 2. Load Optimization

3.3. Experimental research on displacement measurement

Once the optimal loading scheme has been ascertained, with the assumption that the damaged bars retain 70% of the maximum predicted stiffness, the optimal loading strategy for the horizontal bars serves as a blueprint for further investigation. Initially, the identified optimal loading scheme is implemented, and the requisite a priori data is gleaned through horizontal and vertical displacement measurements across the entire nodal network. The overall nodal displacement under load conditions is calculated to facilitate subsequent investigations into the underlying patterns. Subsequently, the ensuing process mirrors that of static loading experimental inquiries. The established optimal loading scheme is leveraged to generate 10,000 stochastic stiffness values for bars 3-4 and 3-8, respectively, following a uniform distribution model for the impaired bars. These sampled data points are then integrated into the likelihood function for computational analysis utilizing the formula.

DOI: 10.54254/2755-2721/72/20241053

$$e^{-\frac{\frac{1}{2}(\text{simulated value}-\text{priori value})^2}{0.0005}} \quad (4)$$

The variables encompass distinct measurement nodes, measurement orientations, and the frequency of measurements, contributing to a comprehensive evaluation of the varying conditions of structural behavior. The Monte Carlo rejection sampling technique was invoked to sieve through the samples and compile the data output. The dataset encapsulates the count of accepted samples and the corresponding stiffness values of the bars for which the samples were approved. Subsequently, the data was transposed into Excel for further processing, employing the RMSE difference methodology. A smaller RMSE difference heralds a more optimal outcome. Post this, the comprehensive node horizontal-vertical optimal loading program underwent sampling simulation, culminating in the optimal RMSE difference data for comparative analysis. Striving for utmost efficiency, the objective was to minimize the number of measurement parameters while achieving a proximity to the optimal RMSE difference. Leveraging diverse measurement programs loaded onto the node facilitated identifying an integrated optimal measurement program, potentially offering streamlined and precise insights into the dynamics. Initially, the exploration commences with single-node unidirectional displacement measurements, bifurcated into two schemes, each encompassing six distinct cases. The first scheme entails single-node horizontal direction measurements, while the second scheme focuses on single-node vertical direction measurements. The inquiry then transitions to two-node measurements, delineated into three scenarios. The initial two scenarios entail 15 cases each, with the third scenario comprising 30 cases. The scenarios include: 1. Two-Node Horizontal Direction Measurement 2. Two-Node Vertical Direction Measurement 3. Two-Node Combination Measurement, incorporating one horizontal and one vertical direction. Subsequently, the investigation progresses to multi-node and multi-parameter measurements, enhancing the elucidation and validation of the previously established principles. The optimal measurement scheme is extrapolated, highlighting the most effective approach for measuring node 3's vertical displacement, node 7's vertical displacement, and node 4's lateral displacement, resulting in a RMSE difference of 0.037. This signifies a 33% decrease compared to the comprehensive horizontal-vertical measurement encompassing 12 parameters, showcasing a minimal RMSE difference of 0.027. This optimized strategy achieves a 75% reduction in measurement expenditures and attains a remarkable accuracy of 72%.

4. Law analysis and experimental conclusions

The experimental data is compiled and summarized for meticulous data processing and comparative analysis. Initially, the experiment scrutinizes the attributes of diverse static loading programs to discern the fundamental principles at play. The root-mean-square difference across different measurement schemes is meticulously assessed in the subsequent phase to pinpoint the optimal measurement strategy.

4.1. Analysis of the First Step Experimental Law

During the initial phase of the experiment, seven noteworthy observations were deduced from the distinct loading schemes:

(1) When a singular load is vertically applied, the direction of loading exhibits minimal influence on the data outcomes, particularly in the vertical loading scenario. The impact of the loading direction on the final acceptances and histograms was negligible, resulting in virtually indistinguishable results.

(2) Vertical loading with a single load divulges an intriguing updating effect, showcasing favorable outcomes for horizontal bars 3-4 but adverse effects for diagonal bars 3-8.

(3) Engaging in single load vertical loading led to disparate updating results between absolute and relative errors. Although the relative error's acceptances surpassed the absolute error's, the overall image distribution remained largely consistent.

(4) When subjected to single load horizontal loading, the established laws mirrored those observed in single load vertical loading, particularly the first three laws. Nonetheless, the updated outcomes were less optimal compared to the vertical loading scenario. Figure 3 meticulously delineates the distinct impacts of varied loading approaches on the crossbar at a singular loading node. The horizontal axis depicts stiffness (EA/10^5 KN·m^2), while the vertical axis portrays the acceptance count. The left side

DOI: 10.54254/2755-2721/72/20241053

showcases vertical loading effects, while the right side illustrates loading influences. In the double-loaded isotropic vertical loading scenario, the governing principles align with the preceding two cases. Notably, the updating effect on horizontal bar 3-4 emerges as the most pronounced, culminating in the optimal loading of this horizontal bar within the experimental framework (Fig. 2).

The observed laws mirror the previous scenarios after implementing double-loaded isotropic horizontal loading. However, the horizontal bar manifests a more substantial updating effect compared to single-loaded horizontal loading, albeit less pronounced than in the double-loaded through-vertical loading case.

In the double-loaded isotropic vertical loading context, the identified law corresponds to the patterns observed in the previous scenarios. For example, the loading configuration of two nodes up and three nodes down mirrors the effects of loading two nodes down and three nodes up, with the latter yielding more favorable updating outcomes. Notably, optimal diagonal bar loading configuration results are attained by loading two nodes up and three nodes down, as illustrated in Fig. 2.

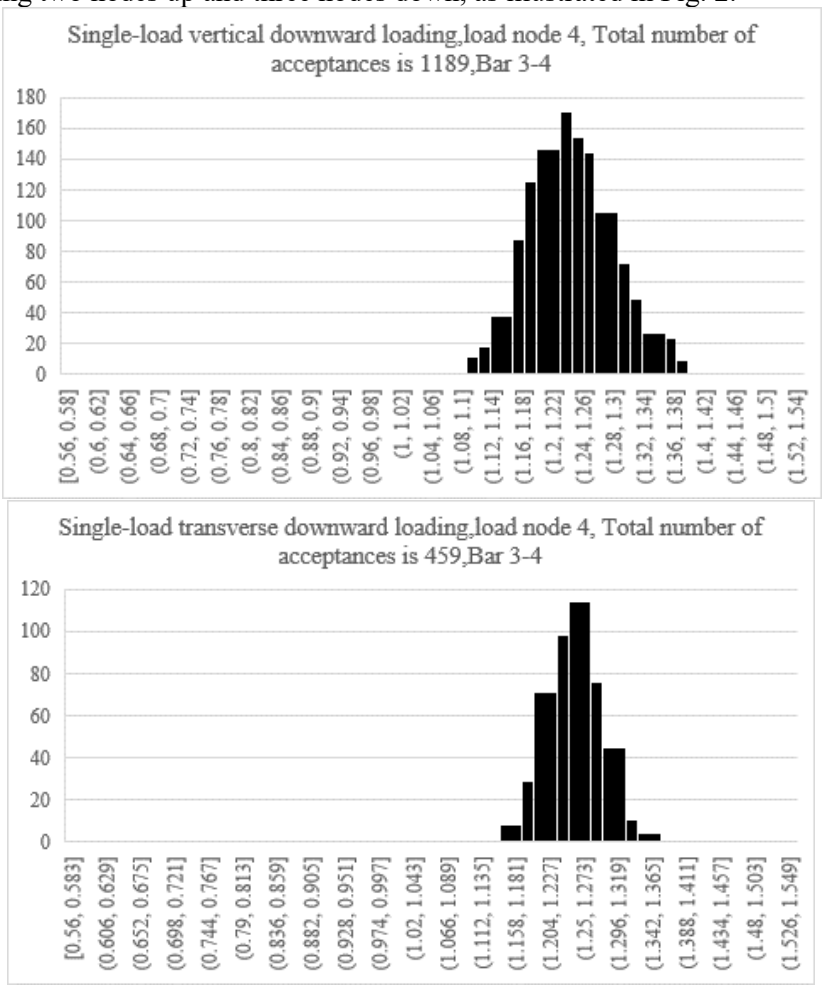

Figure 3. Comparison of different loading effects

4.2. Analysis of the law of the second step of the experiment

In the second phase of the experiment, a multitude of insights were gleaned from diverse measurement schemes. Firstly, it was deduced that the quality of optimized data improves with an increased number of detected nodes and measured parameters. This observation resonates with the principle of diminishing marginal benefit. Notably, in a specific instance where three parameters were optimized, including measurements from node 3 vertically, node 7 horizontally, and node 4 horizontally, a result of 0.037

DOI: 10.54254/2755-2721/72/20241053

was achieved, representing 72% of the optimal effect. Optimizing six parameters resulted in a value of 0.033, achieving 81% of the best effect.

Secondly, an intriguing trend emerged indicating that when focusing solely on vertical displacement, the effectiveness of single measurement point, double measurement point, and all six measurement points surpassed that of horizontal displacement considerations. Moreover, it was observed that the magnitude of displacement at the measurement node directly correlated with the intensity of the updating effect, with the most significant effect achieved when measuring vertical displacement at node 7.

Lastly, the combined horizontal and vertical measurements proved more effective than individual horizontal or vertical measurements alone, potentially rivaling the efficacy of measuring additional nodes. The optimal combination of two nodes yielded a result of 0.043, while the most effective single-direction combination resulted in a value of 0047.

4.3. Conclusion of the Study

When measurement points span all nodes and horizontal-vertical displacements are determined, loading can be executed in alignment with the equivalent beam law. For a horizontal bar, the focus lies on maximizing the bending moment within the identified section. Conversely, when dealing with an inclined bar, the objective shifts to maximizing the shear force within the specified portion. Consequently, as per the measurement scheme outlined, nodes exhibiting greater displacement yield a more significant updating effect.

Employing combined parameters for measurement proves superior to single-direction measurements, enhancing the accuracy of the analysis. Simultaneously, the structural mechanics principle of virtual work is encapsulated in the equation:

$$\Delta = \sum\left(\frac{N_P \cdot \bar{N}}{EA} l\right) \tag{5}$$

Here, N_P signifies the load magnitude in the loading scheme, while $\bar{N}$ represents the displacement magnitude in the measurement scheme. Notably, a larger Δ value correlates with a more pronounced updating effect. Conversely, when data correlation among nodes is less satisfactory, the updating effect more noticeable.

5. Conclusion

This study introduces a novel Bayesian update-based approach for detecting damage in super-static trusses, offering a more cost-effective and efficient diagnostic method. Utilizing Opensees, the model is structured around two experimental phases. The initial step focuses on determining the optimal loading scheme, while the subsequent stage delves into identifying the ideal measurement scheme based on the optimized loading strategy. Monte Carlo rejection sampling and Bayesian updating techniques are employed for precise calculations.

The findings of this research emphasize the importance of combining measurements to maximize efficiency, resulting in a notable 72% improvement in data accuracy while requiring 75% fewer measurement data points. Furthermore, the experimental outcomes validate the foundational principles of virtual work. Notably, when assessing damage in practical truss bridges, it is advised to prioritize the construction of a model featuring structural elements. Subsequently, the loading scheme with the maximum bending moment of the measured transverse member should be implemented. Conversely, if the measured member is a diagonal bar, the loading scheme exhibiting the greatest shear force of the measured section should be employed. Moreover, the model should be meticulously devised to pinpoint nodes displaying the most substantial displacements, which can be extrapolated to the physical structure. This methodology presents a promising avenue for attaining precise measurement outcomes without on cost-effectiveness.

References

[1] Housner G W, Bergman L A, Caughey T K, et al 1997 J. Engineering Mechanics 123(9) p 897-971.

DOI: 10.54254/2755-2721/72/20241053

[2] Gao Y B 2015 Improvement and application of structural damage identification method based on Bayesian model updating Institute of Engineering Mechanics, China Earthquake Administration p 1.
[3] Hou Y F 2012 Damage detection of ancient timber structures under random excitation based on amplitude vector of cross-correlation function D Xi 'an University of Architecture and Technology p 1-2
[4] Rytter A 1993 Vibrational based inspection of civil engineering structures Department of Building Technology and Structural Engineering, Aalborg University, Denmark
[5] Geyskens P, Kiureghian A D, Monteiro P 1998 J. of structural engineering 124(1) p 89-95
[6] Wang Yu 2014 Application of Bayesian parameter updating in reliability analysis Nanjing University of Aeronautics and Astronautics
[7] Simoen E, Moaveni B, Conte J P, et al 2013 J. Engineering Mechanics, 139(12) p 1818-1830
[8] Zhang Qinming, Li Quanwang, Li Kefei, etc 2015 Quality control of concrete durability in Hong Kong-Zhuhai-Macao project under chloride environment J Engineering Mechanics 32 (03) p 175-182.
[9] Song Laijian, Wang Jingquan 2018 Research progress on structural damage identification in civil engineering Chinese Society of Civil Engineering. Proceedings of the 2018 annual academic conference of the Chinese society of civil engineering. Key Laboratory of Concrete and Prestressed Concrete Structures, Ministry of Education, Southeast University ; national Prestressed Engineering Technology Research Center of Southeast University p 12.
[10] Beck J L, Katafygiotis L S 1998 J. Engineering Mechanics 124(4) p 455-461.